The Complex X-Ray Spectra of Two High Redshift Quasars Observed with ASCA

Peter SERLEMITSOS and Tahir YAQOOB*

NASA/GSFC, Code 666, Greenbelt, MD 20771, USA

and

Institute of Space and Astronautical Science, 3-1-1 Yoshinodai, Sagamihara, Kanagawa 229

George RICKER and Jonathon WOO

Center for Space Research, Massachusetts Institute of Technology, Cambridge, MA 02139, USA

and

Hideyo KUNIEDA, Yuichi TERASHIMA, and Kazushi IWASAWA

Department of Astrophysics, School of Science, Nagoya University, Chikusa-ku, Nagoya 464-01

Abstract

We report preliminary results of ASCA observations of two high-redshift quasars ($z \sim 3$), PKS 0438−436 and PKS 2126−158. We find spectral flattening towards low energies in both sources, first found with ROSAT and interpreted as being due to excess X-ray absorption. However, the ROSAT data lacked the bandpass and sensitivity to unambiguously support this interpretation. We find that for PKS 2126−158, absorption in intervening low-redshift material along the line-of-sight provides a statistically better description of the data than absorption in material intrinsic to the quasar. The redshift of the putative absorber is required to be less than a few tenths. Given the redshift constraints and the fact that absorption is not common in lower redshift quasars, this result is not easily explained by a simple model. Either the absorber may be complex or else the inrinsic X-ray spectrum may be complex, or both. Compton-reflection dominated models are ruled out but a broken power-law model provides good fits to the data without requiring excess absorption. The break energy is at $\sim$ 6–8 keV in the quasar frame and the energy index of the soft component is required to be extremely flat. This may mean that the X-ray emission in these objects is dominated by synchrotron losses as in BL Lac objects.

Key words: Quasars: individual (PKS 0438−436, PKS 2126−158) — X-rays: galaxies

1. Introduction

The high redshift quasars PKS 0438−436 and PKS 2126−158 were observed with ASCA on 1993 July 13 and 1993 May 16–17 respectively (see table 1). The redshift of $z \sim 3$ for both objects means that the X-ray spectrum can be measured up to $\sim$ 40 keV (quasar frame) with ASCA. The ASCA data provide spectra with the highest sensitivity in such a broad bandpass for quasars at this high a redshift. Both objects are very high luminosity, compact, radio-loud flat-spectrum sources. Both PKS 0438−436 and PKS 2126−158 have been observed twice with the ROSAT Position Sensitive Proportional Counter (PSPC) which measured spectra which could not, for either source, be interpreted as a simple power law plus Galactic absorption (Wilkes et al. 1992; Elvis et al. 1994). Instead, the spectrum of both sources was observed to flatten at low energies (below $\sim$ 1 keV in the

observer's frame) and this was interpreted as being due to excess absorption along the line-of-sight. The PSPC could not constrain the redshift of the absorber and did not warrant investigation of alternative continuum forms. PKS 2126−158 has also been observed by EXOSAT (Ghosh, Soundararajaperumal 1992) which could not however constrain the low energy spectral shape since the Medium Energy (ME) spectra of weak sources are dominated by systematics of background subtraction and the Low Energy instruemnt (LE) has no energy resolution. It is important to try to understand the origin of the spectral flattening because it must inevitably impose constraints on the nature of the central X-ray source and/or its physical environment. It may also have implications for AGN spectral evolution and the Cosmic X-ray Background (CXRB).

---

* With the Universities Space Research Association.

Table 1. Quasar properties and ASCA count rates.

Quasar	z	N_H $(10^{21}\,cm^{-2})$	V	SIS 0 $cts\,s^{-1}$	SIS 1 $cts\,s^{-1}$	GIS 2 $cts\,s^{-1}$	GIS 3 $cts\,s^{-1}$
PKS 0438−436	2.852	0.150*	18.8	0.011	0.006	0.017	0.021
PKS 2126−158	3.275	0.485†	17.3	0.081	0.066	0.068	0.085

* Galactic absorption, Stark et al. 1992.
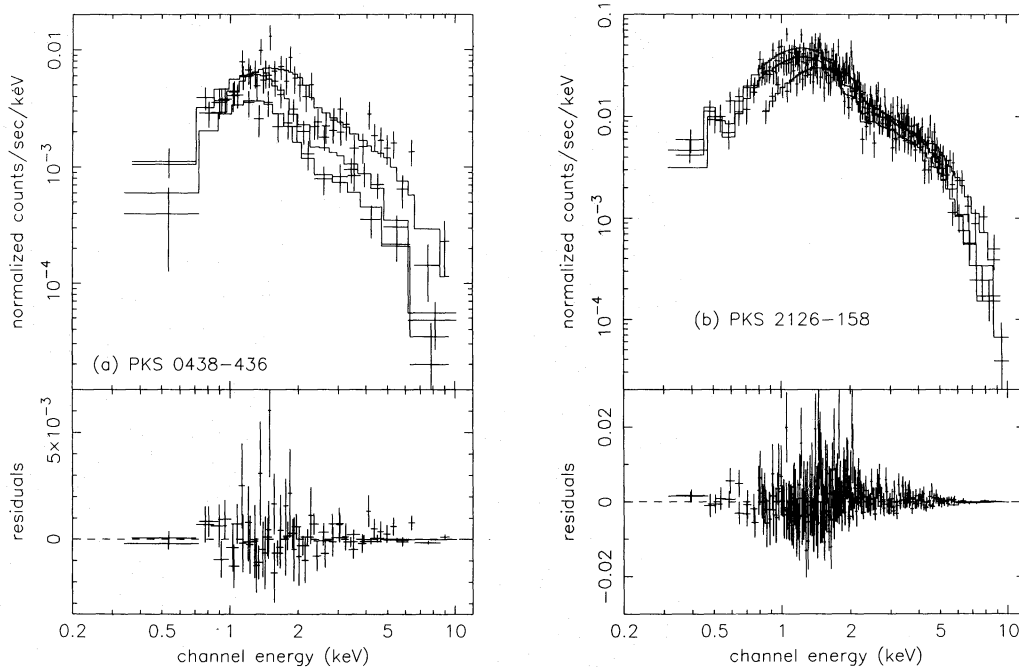† Galactic absorption, Elvis et al. 1989.

Fig. 1. The data, best-fitting model, and residuals for (a) PKS 0438−436 and (b) PKS 2126−158 when the model is a simple power law plus absorber at $z = 0$.

2. The ASCA Data

ASCA has four identical thin-foil, light-weight X-ray telescopes (XRT) which focus X-rays onto one of two Solid-state Imaging Spectrometers (SIS) or one of two Gas Imaging Spectrometers (GIS, see Ohashi et al. 1991). See Tanaka et al. (1994) for a summary of the ASCA mission and focal-plane detectors. The SIS was operated in 4-CCD mode for PKS 0438−436 and 1-CCD mode for PKS 2126−158. Table 1 shows the raw count-rates for each source and each sensor (hereafter the two SIS sensors are referred to as S0 and S1 and the two GIS sensors as S2 and S3).

Spectra were extracted from each sensor from a circular region centred on the source. Typical radii were $\sim 1'.5$ for SIS and $\sim 2'.5$–$3'.5$ for GIS. For S0 and S1 a background spectrum was extracted from a thin annulus centered on the same point as the source region but with much larger radii, restricting contamination from the source to a few percent of the counts in the background region. For the GIS a background spectrum was obtained from an offset circular region about the same size as the source. In S0 and S1 the source counts for PKS 0438−436 were split between 2-CCD chips and the events from the source region in both chips were combined to give a single spectrum for each of S0 and S1. In reality, none of the SIS chips have an identical energy response so that technically the events from different chips should be treated separately. However, in this case counting statistics easily dominate over systematic differences in the CCD chips. All spectra were binned so that there was a minimum of 20 counts per energy bin. This allows us to use the χ^2 minimization technique in the spectral fitting process. At the time of writing the energy response and position-dependent gain calibration for S3

Table 2. Spectral fitting results.

Model	Parameter	PKS 0438−436	PKS 2126−158
1	Γ	1.70 (1.52–1.90)	1.63 (1.54–1.71)
	N_H (10^{21} cm^{-2})	2.02 (1.14–3.15)	1.46 (1.09–1.87)
	χ^2/d.o.f.	62.3/67	218.6/249
2	Γ	see text	1.62 (1.53–1.71)
	N_H (10^{21} cm^{-2})	see text	0.99 (0.61–1.71)
	z	see text	0.027 (0.00–0.44)
	χ^2/d.o.f.	see text	218.5/248
3	Γ_1	0.68 (−0.65–1.08)	1.11 (0.96–1.25)
	Γ_2	1.65 (1.43–1.99)	1.70 (1.58–1.86)
	E_{break} (keV)	1.57 (0.98–2.45)	1.91 (1.53–2.36)
	χ^2/d.o.f.	64.9/66	210.6/248
4	Γ	3.07 (2.69–3.17)	3.07 (3.02–3.12)
	χ^2/d.o.f.	59.1/63	290.0/235

Note.—Values in parentheses indicate 90% confidence intervals for 2 interesting parameters (i.e., $\Delta\chi^2 = 4.605$) for models 1–3 and 1 interesting parameter for model 4 (i.e., $\Delta\chi^2 = 2.706$). The models are (1) power law plus absorption at $z = 0$; (2) power law plus an absorber with z free plus Galactic absorption; (3) broken power law plus Galactic absorption only; (4) Pure Compton reflection plus Galactic absorption only.

was subject to considerable uncertainty and showed discrepant behavior compared to the other three detectors (see also Yaqoob et al. 1994). Therefore, data from this sensor is excluded here. All the spectral fitting described below refers to simultaneous fits with data from the three instruments, unless otherwise stated. Note that for both sources statistical errors dominate over systematics from the three instrumental responses.

3. Spectral Fitting Results

3.1. Absorption Models

Initially we fit the spectra with a simple power law plus local absorption ($z = 0$) in cold material using standard cross-sections from Morrison and Macammon (1983) and solar abundances. Apart from three normalizations, there are two free parameters; namely the photon index, Γ, and the column density, N_H, of the absorber. Good fits are obtained for both sources and the results are shown in table 2 (model 1) and figure 1. The best-fitting power-law photon indices are 1.70 and 1.63 for PKS 0438−436 and PKS 2126−158 respectively and the best-fitting column density exceeds the Galactic value with a high level of significance in each case, the 3-sigma lower limits on N_H being 0.7 and 0.8 × 10^{21} cm^{-2} respectively (compare with the Galactic values in table 1). The best-fitting values of N_H are 2.02 and 1.46 ×10^{21} cm^{-2} for PKS 0438−436 and PKS 2126−158 respectively. For

comparison, the ROSAT data gave a best-fitting photon index of 1.70 for both quasars and column densities of 0.7 and 1.3 ×10^{21} cm^{-2} for PKS 0438−436 and PKS 2126−158 respectively (Elvis et al. 1994). It is not clear whether the differences in N_H (about a factor of 3 for PKS 0438−436) are a result of the different instrumental bandpass and resolution or represent a real spectral change. This will be investigated in the future. Note that there was no apparent spectral variability between the two ROSAT observations of either source; the two observations of each source were separated by over 1.5 yr. We checked whether the apparent excess column density could be due to overestimating the background level by repeating the fits with the normalization of the background reduced by a factor of 2 (rather extreme). We obtained 90% lower limits on N_H of 1.0 and 0.9 × 10^{21} cm^{-2} for PKS 0438−436 and PKS 2126−158 respectively, still well in excess of the Galactic values.

For PKS 0438−436 we estimate the observed flux (0.1–2.5 keV) to be 4.5×10^{-13} erg cm^{-2} s^{-1}, consistent with the 'wobbled' PSPC observation in 1992 and an Einstein observation in 1979 (see Elvis et al. 1994). For PKS 2126−158 we estimate the 0.1–2.5 keV flux to be 2.3×10^{-12} erg cm^{-2} s^{-1}, compared with 3.7×10^{-12} erg cm^{-2} s^{-1} obtained from the PSPC (Elvis et al. 1994). Further work is required to quantify the uncertainties and determine whether the apparent change is real. These ASCA fluxes are lower limits and involve extrapolation of the model to 0.1 keV. From the ASCA data we estimate lower limits on the 2–10 keV unabsorbed luminosities in the quasar frame of ~ 1.2 and $\sim 9.5 \times 10^{47}$ erg s^{-1} for PKS 0438−436 and PKS 2126−158 respectively ($H_0 = 50$ km s^{-1} Mpc^{-1} and $q_0 = 0$).

Next we let the redshift of the absorber float, including Galactic absorption at $z = 0$. Unfortunately the counting statistics for PKS 0438−436 are insufficient to constrain the redshift of the putative absorber. In fact there are local minima in χ^2 for several values of z between 0.0 and 2.852 and the differences in the minimum χ^2 values are insignificant. Thus we give the best-fitting parameters (table 2, model 2) for PKS 2126−158 only since there is no unique solution for PKS 0438−436. On the other hand, figure 2 shows the contours in the z–N_H plane for confidence levels of 68%, 90%, and 99% (2 interesting parameters) for both sources. For PKS 2126−158 it can be seen that a local absorber, with low redshift, is strongly preferred. Intrinsic absorption at the redshift of the quasar is in fact formally excluded at the 99% level. We also tried replacing the power law with a thermal bremsstrahlung continuum which also gave good fits. With the absorber at $z = 0$, the best-fitting values of the temperature, kT, are ~ 35 and ~ 45 keV for PKS 0438−436 and PKS 2126−158 respectively and are not very sensitive to z. With this continuum, intrinsic
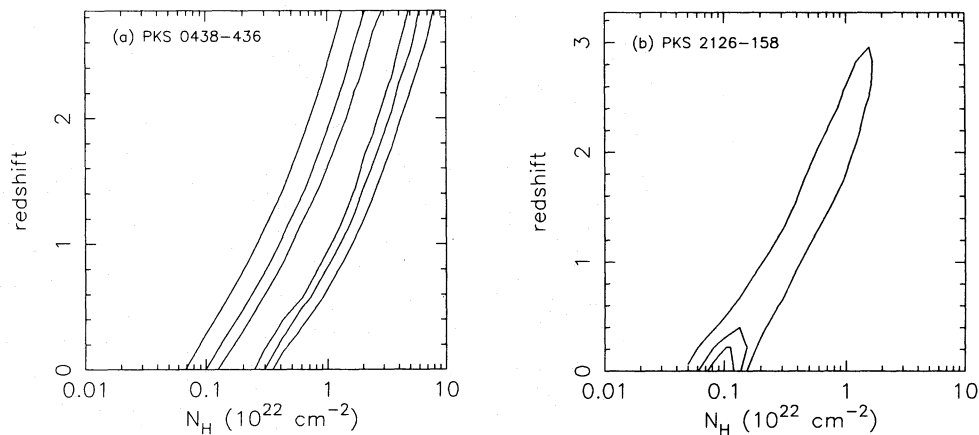
Fig. 2. The contours in the z–N_H plane, corresponding to confidence levels of 68%, 90%, and 99% (2 interesting parameters, see Lampton et al. 1976), when the model is a simple power law plus absorption, with the redshift of the absorber as a free parameter. The model contains an additional absorber with column density fixed at the Galactic value.

absorption can no longer be excluded at the 99% level but local absorption is still statistically preferable. In passing, we note that these temperatures are similar to the temperature of ~ 40 keV obtained when the ~ 3–100 keV CXRB is fitted with a thermal model (Marshall et al. 1980).

3.2. Complex Continuua

Here we investigate continuum models which can fit the data with *Galactic absorption only*. First we try a broken power law model where the continuum below a certain energy, E_{break}, has a photon index Γ_1 and a photon index Γ_2 above this energy so that there are now three free parameters (plus normalizations). Good fits are again obtained and the results are shown in table 2 (model 3). The best-fitting break energies are, in the quasar frame, ~ 6 keV for PKS 0438−436 and ~ 8.2 keV for PKS 2126−158. It is important to note that the spectra below the break energy are required to be extremely flat, the energy index for PKS 0438−436 actually being negative and that for PKS 2126−158 nearly zero. This may be indicative of an emission mechanism due to synchrotron losses and may not be so unexpected given the radio power of both objects. The very high X-ray luminosities, in excess of $\sim 10^{47}$ erg s^{-1}, may be indicative of strongly beamed emission. The X-ray spectra of BL Lac objects can in fact be interpreted in terms of a broken power-law spectrum (e.g., see Madejski, Schwartz 1988) except that the apparent break energy is at much lower energies (~ 1.5 keV).

Next we try a 'pure' Compton-reflection model which is very flat below ~ 10 keV (e.g., White et al. 1988; George, Fabian 1991). Such a model, where the X-ray spectra of AGN at high redshifts are dominated by a

Compton-reflection component from optically thick matter, has been invoked to account for the spectrum of the CXRB from ~ 3 keV to beyond 1 MeV (e.g., Fabian et al. 1990). In that case, for the sources which make a dominant contribution to the X-ray background, the fraction of the direct (assumed power law) continuum allowed to escape is required to be less than $\sim 10\%$. Here, we set the escaping continuum fraction to zero to minimize the number of free parameters. The model then has only 1 free parameter, Γ (plus normalizations). Similar values for the best-fitting photon index ($\Gamma \sim 3$; see table 2, model 4) are obtained for both sources. However, the fit for PKS 2126−158 is *not* acceptable at the 99% level. This is because the model predicts a large redshifted Fe-K absorption edge which is not present in the data. One can obtain an adequate fit if the iron abundance is reduced to about a tenth of solar and a small fraction of the direct continuum is allowed to escape but then the increase in the number of free parameters does not make the model statistically preferable to a simple power law plus absorption.

Note that in the above Compton-reflection model we would expect to observe a redshifted Fe-K line from fluorescence in the reflecting medium. However, the data show no evidence for a significant redshifted Fe-K line. Using the data from S0 (the SIS in which the sources are closest to the XRT optical axis), we place formal, 90% confidence upper limits (1 interesting parameter) on the equivalent width (in the quasar frame) of a narrow, Gaussian 6.4 keV line (intrinsic width 0.1 keV) of 256 eV and 140 eV for PKS 0438−436 and PKS 2126−158 respectively. For a spectrum dominated by reflection, one would expect a much larger equivalent width, of the order of 1 keV (e.g., George, Fabian 1991).

4. Discussion

Both PKS 0438−436 and PKS 2126−158 exhibit convex spectral curvature, which if interpreted as excess absorption, for the case of PKS 2126−158, absorption in intervening low-redshift material in the line-of-sight provides a statistically better description of the data than absorption in material intrinsic to the quasar. For both sources, intrinsic absorption is not required. Thus, at least for PKS 2126−158, the interpretation of the spectral flattening as X-ray absorption due to material associated with a cluster cooling flow is not favorable. If the apparent excess absorption in these objects occurs in intervening material, as is statistically preferable for at least one of them, then damped Lyα disk absorption systems with typical column densities of $\sim 10^{20-21}$ cm^{-2} (Turnshek et al. 1989) are likely candidates. Neither of the two quasars shows intervening damped Lyα absorption at $z > 1.88$ (Morton et al. 1978; Sargent et al. 1990; Lanzetta et al. 1987) so the redshift of any absorber must be less than this. However, given the number density per unit redshift interval of such absorbers, the expected number in the interval $z = 0$ to 0.5 is only $\sim 0.023-0.087$ (e.g., see Elvis et al. 1994). This estimate is based on an extrapolation because the density of damped Lyα systems below $z = 2$ is unknown. So, these considerations, together with the fact that excess absorption is *not* common in low-redshift quasars (Wilkes, Elvis 1987; Worrall, Wilkes 1990) means that the interpretation of the spectral flattening in both of the quasars studied here, as excess absorption in cold, uniform, solar abundance material is difficult to reconcile with the data. Therefore, alternatives must be seriously considered.

One possibility is that the absorption is complex. Preliminary work suggests that if the absorbing material only partially covers the source or is ionized or has nonsolar abundances, the absorber is allowed to be at higher redshifts. More details will be presented in a future paper. Another possibility is that the spectral curvature is a property of the intrinsic X-ray emission. Again, further work is required to investigate possible models in more detail but at present, it appears that the emission mechanism may be dominated by synchrotron losses. We can rule out Compton reflection as the dominant spectral component on the basis of the lack of an observed Fe-K edge and redshifted Fe-K emission line (the intrinsic quasar luminosities would also have to be orders of magnitude higher than observed).

Of the four high-redshift quasars studied by Elvis et al. (1994) (all radio loud with z between 2.852 and 3.384) that had measurable X-ray spectra, two show definite spectral flattening (PKS 0438−436 and PKS 2126−158) and one has a spectrum which is entirely consistent with a power law plus Galactic absorption (Q0420−388). The remaining one (S5 0014 + 81) has possible spectral flat-

tening but the statistical significance of this result is low. Thus we only know that the X-ray spectral property shared by PKS 0438−436 and PKS 2126−158 is not a function of redshift alone. It will be important to observe many more high-redshift AGN with ASCA to determine how common the spectral flattening observed in PKS 0438−436 and PKS 2126−158 is and whether the phenomenon can be correlated with any other properties of the objects. This will help to determine whether the spectral flattening is indeed an intrinsic property of the source (and if so provide clues as to its origin) and also to assess the impact of these objects on the CXRB spectrum.

References

Elvis M., Fiore F., Wilkes B.J., McDowell J. 1994, ApJ in press
Elvis M., Lockman F.J., Wilkes B.J. 1989, AJ 97, 777
Fabian A.C., George I.M., Miyoshi S., Rees M.J. 1990, MNRAS 242, 14p
George I.M., Fabian A.C. 1991, MNRAS 249, 352
Ghosh K.K., Soundararajaperumal S. 1992, A&A 265, 413
Lampton M., Margon B., Bowyer S. 1976, ApJ 208, 177
Lanzetta K.M., Turnshek D.A., Wolfe A.M. 1987, ApJ 322, 739
Madejski G.M., Schwartz D.A. 1988, ApJ 330, 776
Marshall F.E. et al. 1980, ApJ 235, 4
Morrison R., McCammon D. 1983, ApJ 270, 119
Morton D.C., Savage A., Bolton J.G. 1978, MNRAS 185, 735
Ohashi T., Makishima K., Ishida M., Tsuru T., Tashiro M., Mihara T., Kohmura Y., Inoue H. 1991, Proc. SPIE 1549, 9
Sargent W.L.W., Steidel C., Boksenberg A. 1990, ApJ 351, 364
Stark A.A., Gammie C.F., Wilson R.W., Bally J., Linke R.A., Heiles C., Hurwitz M. 1992, ApJS 79, 77
Tanaka Y., Holt S.S., Inoue H. 1994, PASJ 46, L37
Turnshek D.A., Wolfe A.M., Lanzetta K.M., Briggs F.H., Cohen R.D., Foltz C.B., Smith H.E., Wilkes B.J. 1989, ApJ 344, 567
White T.R., Lightman A.P., Zdziarski A.A. 1988, ApJ 331, 939
Wilkes B.J., Elvis M. 1987, ApJ 323, 243
Wilkes B.J., Elvis M., Fiore F., McDowell J.C., Tananbaum H., Lawrence A. 1992, ApJL 393, L1
Worrall D.M., Wilkes B.J. 1990, ApJ 360, 396
Yaqoob T. et al. 1994, PASJ 46, L49